A versatile microelectromechanical system for nanomechanical testing

B. Pant, B. L. Allen, T. Zhu, K. Gall, and O. N. Pierron[a]
*G. W. Woodruff School of Mechanical Engineering, Georgia Institute of Technology, Atlanta,
Georgia 30332-0405, USA*

This letter presents a microelectromechanical system (MEMS) material testing setup that relies on electronic measurements of nanospecimen elongation. Compared to previously demonstrated MEMS that rely on high magnification images to measure elongation, this MEMS is more versatile, allowing *both in situ* and *ex situ* testing of nanomaterials with high accuracy and precision. We describe and characterize the MEMS device and illustrate its mode of operation with a successful *ex situ* uniaxial tensile test of a nanocrystalline nickel nanobeam. The combination of *ex situ* and *in situ* nanomechanical tests will enable a thorough investigation of critical properties pertaining to the reliability of nanosystems. © *2011 American Institute of Physics*. [doi:10.1063/1.3553195]

Microelectromechanical systems (MEMS) were recently described as superior material testing systems (MTS) for nanomaterials.[1] Currently, the most advanced MEMS MTS are best suited for *in situ* scanning electron microscope (SEM) or transmission electron microscope (TEM) studies,[2–7] since they require high magnification images to measure strain. In this letter, we highlight the need for a more versatile MEMS device that allows *both in situ* and *ex situ* testing of nanomaterials. In turn, we describe and characterize a versatile MEMS device and illustrate its mode of operation with a successful *ex situ* uniaxial tensile test of a nanocrystalline (nc) nickel (Ni) nanobeam. We then discuss the extended range of nanomechanical tests that this MEMS device enables and the corresponding nanomaterials properties that can be thoroughly investigated.

Existing MEMS MTS, whether for nanoscale films[8–12] or for one dimensional nanomaterials,[3,4,6,7,13–22] fall into one of the following categories. The first one is limited to the testing of linear elastic materials since load and displacement are calculated based on the same sensing measurement (image-based[14] or electronic[20]). The second category can measure the elastic and inelastic properties of nanomaterials from two independent sensing measurements for load and displacement. The sensing techniques further distinguish these systems: Image-based (requiring high magnification electron images[2,3,6,11,16,18,21,22] or optical images of amplified displacement[17]) or electronic (based on MEMS capacitive sensors[3,4,6] or a commercial nanoindentor[19,23]). The existing MEMS MTS are dedicated either for *in situ* testing (although some do not allow continuous imaging of the specimen due to the sensing schemes[11,12,16,18,21,22]) or *ex situ* testing[17,24] *only*. While *in situ* TEM testing is highly beneficial to investigate fundamental deformation mechanisms,[1,25] we argue that *ex situ* testing of the same nanomaterials may be required to investigate critical mechanical properties that cannot be measured inside a SEM/TEM chamber in a practical manner (see below). The following MEMS device enables *both in situ* and *ex situ* testing.

The MEMS device shown in Fig. 1 is a through-hole silicon structure isolated from the substrate by a 1 μm thick oxide layer. Its overall dimensions (3.5 mm long and 1.5 mm wide) allow *in situ* TEM testing.[1] The device comprises an electrothermal actuator, a heat sink, a gap for the specimen, and two identical capacitive sensors (CS1 and CS2) on each side of the specimen. The two capacitive sensors can be used to electronically measure the specimen gap change, an idea briefly presented in Ref. 5. As clearly demonstrated below, this unique feature enables *ex situ* testing without losing any accuracy in strain measurements compared to *in situ* systems. This device can provide up to 1.6 μm of thermal actuator displacement without any significant increase in specimen temperature ($<10\ ^\circ$C).[26] The device is mechanically disconnected at two other locations than the specimen gap; these extra 4 μm gaps are filled with stiff, electrically insulating epoxy, thereby allowing electrical isolation between the driving and sensing part without affecting the overall device mechanics.[7] The governing equations of the MEMS device are derived based on the lumped mechanical model shown in Fig. 1(d),[5]

$$X_A = X_S + X_{LS} \quad \text{and} \quad F = K_{LS}X_{LS}, \tag{1}$$

where X_A is the actuator displacement, X_S is the specimen elongation, X_{LS} is the deflection of the load sensor, F is the force applied on the specimen and the load sensor, and K_{LS} is the load sensor stiffness (either 38 N/m or 481 N/m).[26] Dur-
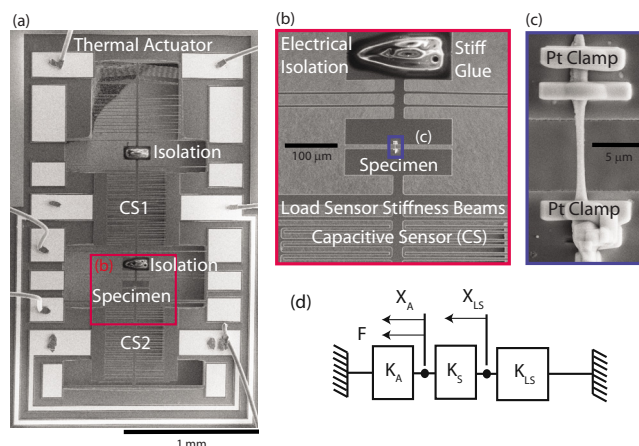

FIG. 1. (Color online) [(a)–(c)] SEM images of the MEMS device and an attached nc Ni nanobeam. (d) Lump model.

[a]Author to whom correspondence should be addressed. Tel.: +1-404-894-7877. Electronic mail: olivier.pierron@me.gatech.edu.
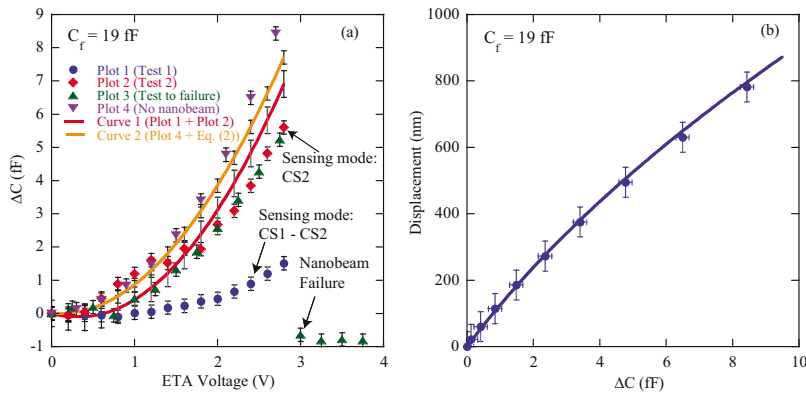
FIG. 2. (Color online) (a) ΔC vs actuator voltage curves for the *ex situ* tensile test of a nc Ni nanobeam. (b) Calibration capacitive sensor displacement vs ΔC curve.

ing a test, X_A is related to the load-free X_A ($X_A^{F=0}$) as follows:[26]

$$X_A = \frac{X_A^{F=0}}{1 + \dfrac{K_{LS}/K_A}{1 + (K_{LS}/K_S)}} \approx \frac{X_A^{F=0}}{1 + (K_{LS}/K_A)} \text{ if } K_{LS} < K_S,$$

(2)

where K_S is the specimen stiffness and K_A is the actuator stiffness ($K_A = 3975$ N/m).[26]

The mode of operation of the MEMS device is illustrated with the uniaxial tensile testing of a nc Ni nanobeam (thickness: 200 nm, width: 700 nm, length: 10 μm, grain size $\sim$20–100 nm)[26] in laboratory air (*ex situ* test). Figure 2(a) shows four experimental plots (measured with an MS3110 chip (Irvine Sensors) with a nominal feedback capacitance $C_f = 19$ fF) and two calculated curves in the form of capacitance change, ΔC versus applied thermal actuator voltage, V. Plots 1–3 represent tensile tests of the same Ni nanobeam (1 and 2 are interrupted prior to failure) while Plot 4 represents a test with no specimen. The sensing mode for the first test (Plot 1) is differential (CS1–CS2) while it is only CS2 for the second test (Plot 2). Plot 3 represents the subsequent test to failure (also CS2 sensing). Curve 1 is the sum of the fitted Plot 1 and Plot 2 corresponding to the CS1 sensing during the test while Curve 2 represents the expected CS1 sensing during the tensile test using Plot 4 and Eq. (2) ($K_{LS} = 481$ N/m). The fact that the two calculated curves closely match confirms that the MEMS' behavior is accurately modeled.[27] Particularly, the difference between X_A and $X_A^{F=0}$ *cannot* be ignored for non negligible K_{LS}/K_A ratios to obtain accurate results. The stress-strain curve shown in Fig.

3(a) is calculated based on Plots 1 and 4 from Fig. 2(a), on Fig. 2(b), representing the calibration curve for the capacitive sensor displacement versus ΔC,[26] and on Eq. (2). The calculated elastic modulus, based on a linear fit of the stress-strain curve, is $E = 208$ GPa. This value is very close to the bulk coarse grain value (210 GPa) and the value measured for nc Ni films with mean grain sizes ranging from 15 to 100 nm (201 ± 15 GPa).[28,29] We therefore conclude that the electronic sensing of specimen elongation allows accurate determination of nanomaterials' mechanical properties based on *ex situ* tests. The accuracy in strain calculation with this technique requires rigid platinum clamps to grip the nanobeam onto the MEMS,[26] which appears to be the case based on SEM images taken before and after the test [see Fig. 3(b)]. We also note that the nanobeam failed with little or no plastic deformation [see Fig. 3(b)], a known result for nc metals.[30] The failure stress is $\sigma_f = 2.3 \pm 0.2$ GPa, confirming that nc Ni is ultrastrong.[31]

Although accurate, the measurements shown in Fig. 3(a) are not highly precise.[32] The precision in displacement measurement was significantly improved by changing the MS3110 configuration from $C_F = 19$ fF to $C_F = 399$ fF. Figure 4(a) shows the calibration curves for the capacitive sensor displacement versus ΔC with $C_f = 399$ fF for two types of capacitive sensors (4 μm versus 2.5 μm gaps), which match very well with the analytical curves.[33] With a noise floor of 0.05 fF [see Fig. 4(b)], the displacement resolution can be as good as 0.25 nm. We therefore conclude that this MEMS device can allow highly accurate *and* precise measurements.

We conclude on the extended capability offered by this versatile MEMS device. First, it can allow continuous imag-
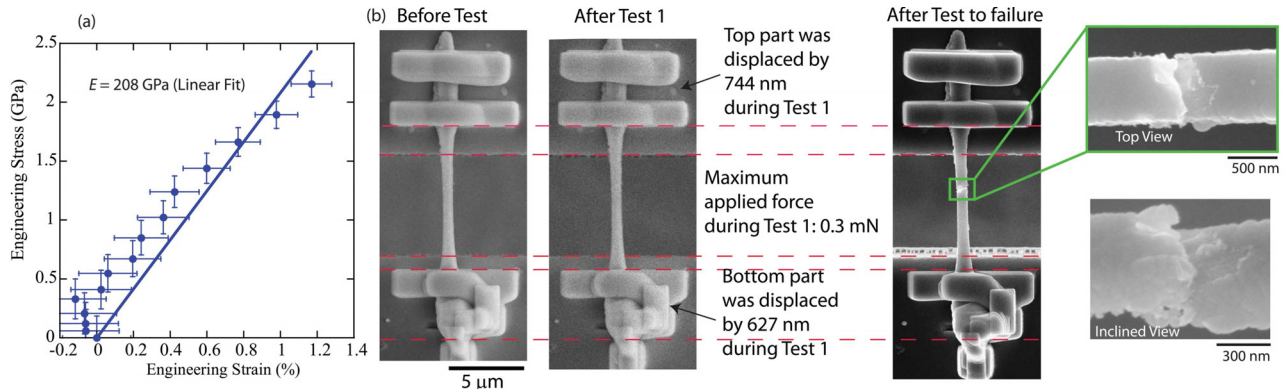

FIG. 3. (Color online) (a) Stress-strain curve calculated based on data shown in Fig. 2. (b) SEM images of the nanobeam before and after tests.
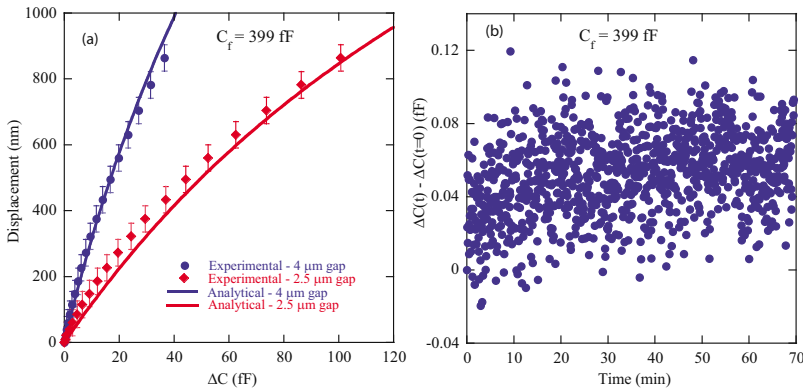
FIG. 4. (Color online) (a) Capacitive sensor displacement vs ΔC curve for two types of capacitive sensor structures. The analytical curves were plotted assuming an etch bias of 0.2 μm. (b) ΔC drift over 1 h testing period.

ing of the specimen during *in situ* TEM testing since load and displacement are both measured electronically. More importantly, it allows the investigation of critical properties pertaining to the reliability of nanosystems, thanks to the *ex situ* testing capability. For example, environment-, time- and cycle-dependent degradation properties (e.g., stress-assisted corrosion, creep, and fatigue) can be continuously measured in an environmental chamber (e.g., controlled humidity and temperature), thanks to the MEMS device apparent stability [see Fig. 4(b)]. *In situ* TEM testing can be periodically performed on interrupted *ex situ* tests to observe microstructural changes in the nanospecimens, with a compatible testing platform. It is expected that the combination of *ex situ* and *in situ* nanomechanical tests will enable a thorough investigation of the aforementioned properties at the nanoscale.

[1]M. A. Haque, H. D. Espinosa, and H. J. Lee, MRS Bull. **35**, 375 (2010).
[2]R. Agrawal, B. Peng, and H. D. Espinosa, Nano Lett. **9**, 4177 (2009).
[3]Y. Zhu and H. D. Espinosa, Proc. Natl. Acad. Sci. U.S.A. **102**, 14503 (2005).
[4]Y. Zhu, N. Moldovan, and H. D. Espinosa, Appl. Phys. Lett. **86**, 013506 (2005).
[5]H. D. Espinosa, Y. Zhu, and N. Moldovan, J. Microelectromech. Syst. **16**, 1219 (2007).
[6]D. F. Zhang, J. M. Breguet, R. Clavel, V. Sivakov, S. Christiansen, and J. Michler, J. Microelectromech. Syst. **19**, 663 (2010).
[7]D. F. Zhang, W. Drissen, J. M. Breguet, R. Clavel, and J. Michler, J. Micromech. Microeng. **19**, 075003 (2009).
[8]M. A. Haque and M. T. A. Saif, J. Microelectromech. Syst. **10**, 146 (2001).
[9]M. A. Haque and M. T. A. Saif, Exp. Mech. **42**, 123 (2002).
[10]M. T. A. Saif and N. C. MacDonald, Sens. Actuators, A **52**, 65 (1996).
[11]S. Kumar, M. A. Haque, and H. Gao, Appl. Phys. Lett. **94**, 253104 (2009).
[12]M. A. Haque and M. T. A. Saif, Proc. Natl. Acad. Sci. U.S.A. **101**, 6335 (2004).
[13]J. J. Brown, J. W. Suk, G. Singh, A. I. Baca, D. A. Dikin, R. S. Ruoff, and V. M. Bright Sens. Actuators, A **155**, 1 (2009).
[14]S. B. Lu, Z. Y. Guo, W. Q. Ding, and R. S. Ruoff, Rev. Sci. Instrum. **77**, 056103 (2006).
[15]S. N. Lu, D. A. Dikin, S. L. Zhang, F. T. Fisher, J. Lee, and R. S. Ruoff, Rev. Sci. Instrum. **75**, 2154 (2004).
[16]S. N. Lu, Z. Y. Guo, W. Q. Ding, D. A. Dikin, J. Lee, and R. S. Ruoff, Rev. Sci. Instrum. **77**, 125101 (2006).
[17]M. Kiuchi, S. Matsui, and Y. Isono, J. Microelectromech. Syst. **16**, 191 (2007).
[18]D. F. Zhang, J. M. Breguet, R. Clavel, L. Philippe, I. Utke, and J. Michler, Nanotechnology **20**, 365706 (2009).
[19]Y. Ganesan, Y. Lu, C. Peng, H. Lu, R. Ballarini, and J. Lou, J. Microelectromech. Syst. **19**, 675 (2010).
[20]A. Corigliano, L. Domenella, and G. Langfelder, Exp. Mech. **50**, 695 (2010).
[21]Q. H. Jin, Y. L. Wang, T. Li, X. X. Li, and F. F. Xu, Sci. China, Ser. E: Technol. Sci. **51**, 1491 (2008).
[22]S. Kumar, D. Zhuo, D. E. Wolfe, J. A. Eades, and M. A. Haque, Scr. Mater. **63**, 196 (2010).
[23]While the use of a nanoidentor yields high-precision measurements, the technique described in Ref. 19 does not appear to be accurate based on the results shown in that paper, whereby the Young's modulus of 200–300 nm Ni nanowires was measured to be 75% lower than the expected value.
[24]The MEMS used in Ref. 17 can be used inside a SEM; however, the sensing technique would not allow continuous imaging of the specimen.
[25]M. Legros, D. S. Gianola, and C. Motz, MRS Bull. **35**, 354 (2010).
[26]B. Pant, S. Choi, E. K. Baumert, B. L. Allen, S. Graham, K. Gall, and O. N. Pierron, "MEMS-based nanomechanics: influence of MEMS design on test temperature," Exp. Mech. (submitted).
[27]The small discrepancy between Curves 1 and 2 may result from the fact that K_A was calculated based on an analytical formula given in Ref. 4.
[28]X. F. Zhang, T. Fujita, D. Pan, J. S. Yu, T. Sakurai, and M. W. Chen, Mater. Sci. Eng., A **527**, 2297 (2010).
[29]Based on X-ray diffraction data not shown here, our nc Ni is slightly more textured [in the (111) direction] compared to Ref. 28 [intensity ratio between (200) and (111) is ~0.15 for our nc Ni, while it is ~0.4 for Ref. 28].
[30]M. Dao, L. Lu, R. J. Asaro, J. T. M. De Hosson, and E. Ma, Acta Mater. **55**, 4041 (2007).
[31]T. Zhu and J. Li, Prog. Mater. Sci. **55**, 710 (2010).
[32]Error bars in displacement measurements from 15 to 25 nm.
[33]This was not the case for nominal C_f=19 fF; however, this did not affect the stress-strain curve measurement since optical calibration was also performed.